Original Article

Insulin-like growth factor 1 stimulates the angiogenic activity of adipose tissue–derived microvascular fragments

Journal of Tissue Engineering
Volume 10: 1–11

DOI: 10.1177/2041731419879837
journals.sagepub.com/home/tej
SAGE

Matthias W Laschke, Elena Kontaxi, Claudia Scheuer, Alexander Heß, Philipp Karschnia and Michael D Menger

Abstract

Angiogenesis in adipose tissue is promoted by insulin-like growth factor 1 signaling. We analyzed whether this regulatory mechanism also improves the angiogenic activity of adipose tissue–derived microvascular fragments. Murine adipose tissue–derived microvascular fragments were cultivated for 24 h in the University of Wisconsin (UW) solution supplemented with vehicle, insulin-like growth factor 1, or a combination of insulin-like growth factor 1 and insulin-like growth factor–binding protein 4. Subsequently, we assessed their cellular composition, viability, proliferation, and growth factor expression. Moreover, cultivated adipose tissue–derived microvascular fragments were seeded onto collagen–glycosaminoglycan scaffolds, which were implanted into dorsal skinfold chambers to study their vascularization and incorporation. Insulin-like growth factor 1 increased the viability and growth factor expression of adipose tissue–derived microvascular fragments without affecting their cellular composition and proliferation. Accordingly, scaffolds containing insulin-like growth factor 1–stimulated adipose tissue–derived microvascular fragments exhibited an enhanced in vivo vascularization and incorporation. These positive insulin-like growth factor 1 effects were reversed by additional exposure of adipose tissue–derived microvascular fragments to insulin-like growth factor–binding protein 4. Our findings indicate that insulin-like growth factor 1 stimulation of adipose tissue–derived microvascular fragments is suitable to improve their vascularization capacity.

Keywords

Tissue engineering, microvascular fragments, insulin-like growth factor 1, insulin-like growth factor–binding protein 4, angiogenesis, vascularization, scaffold

Date received: 17 July 2019; accepted: 12 September 2019

Introduction

The successful engraftment and survival of tissue-engineered constructs crucially depend on the establishment of an adequate blood supply after their implantation.[1,2] To achieve this, the seeding of scaffolds with adipose tissue–derived microvascular fragments (ad-MVFs) represents a promising approach.[3] Ad-MVFs are obtained by short-term enzymatic digestion of fat samples,[4] in contrast to the so-called stromal vascular fraction (SVF), which results from longer digestion times and, thus, consists of a mixture of single endothelial cells, perivascular cells, inflammatory cells, and stem cells,[5,6] Ad-MVFs are fully functional vessel segments.[7] Accordingly, they reassemble much faster into dense microvascular networks within implanted scaffolds and rapidly develop interconnections to the surrounding host microvasculature.[8]

It is conceivable that in a future clinical scenario, autologous ad-MVFs are isolated from liposuctioned fat, immediately seeded onto a scaffold, and retransferred into the tissue defect of a patient during an intraoperative one-step procedure. On the other hand, it is also possible to cryopreserve

Institute for Clinical & Experimental Surgery, Saarland University, Homburg/Saar, Germany

Corresponding author:
Matthias W Laschke, Institute for Clinical & Experimental Surgery, Saarland University, D-66421 Homburg/Saar, Germany.
Email: matthias.laschke@uks.eu

ad-MVFs,[9] which offers the exciting opportunity to store them for later use in biobanks as off-the-shelf vascularization units. In addition, we could demonstrate that ad-MVFs can be precultivated for 24 h prior to scaffold seeding and implantation without affecting their physiological vessel morphology.[10] By using the University of Wisconsin (UW) solution instead of conventional cell culture medium, this can be performed under xeno-free conditions according to good manufacturing practices.[11] Of interest, the short-term cultivation of ad-MVFs is suitable for their stimulation with pro-angiogenic factors, such as erythropoietin, to further boost their subsequent in vivo vascularization capacity.[12]

There is an accumulating body of evidence that the microvasculature of adipose tissue underlies different angiogenic regulatory mechanisms when compared to that of other tissue types. An upregulated expression of hypoxia-inducible factor (HIF)-1α rather promotes fibrosis than angiogenesis in adipose tissue.[13] In contrast, metabolically driven signals associated with an increased caloric intake stimulate the development of new blood vessels.[14] This is most probably due to the fact that the growth of adipose tissue is determined by the proliferative activity of its microvasculature.[15] In this context, Gealekman et al.[16] reported that insulin enhances angiogenesis in adipose tissue, which is mediated by an increased adipocytic secretion of insulin-like growth factor (IGF)-1 and the activation of its receptor on SVF cells.

Based on these findings, we hypothesized in the present study that the stimulation of ad-MVFs with IGF-1 during short-term cultivation improves their vascularization potential. To test this, we cultivated ad-MVFs from donor mice for 24 h in the UW solution, which was supplemented with vehicle, IGF-1, or a combination of IGF-1 and insulin-like growth factor–binding protein 4 (IGFbp4). IGFbp4 inhibits the interaction of IGF-1 with its receptor[16] and, thus, served herein as a negative control. The cellular composition, viability, proliferation, growth factor expression, and vascularization capacity of the cultivated ad-MVFs were analyzed in a panel of in vitro and in vivo experiments.

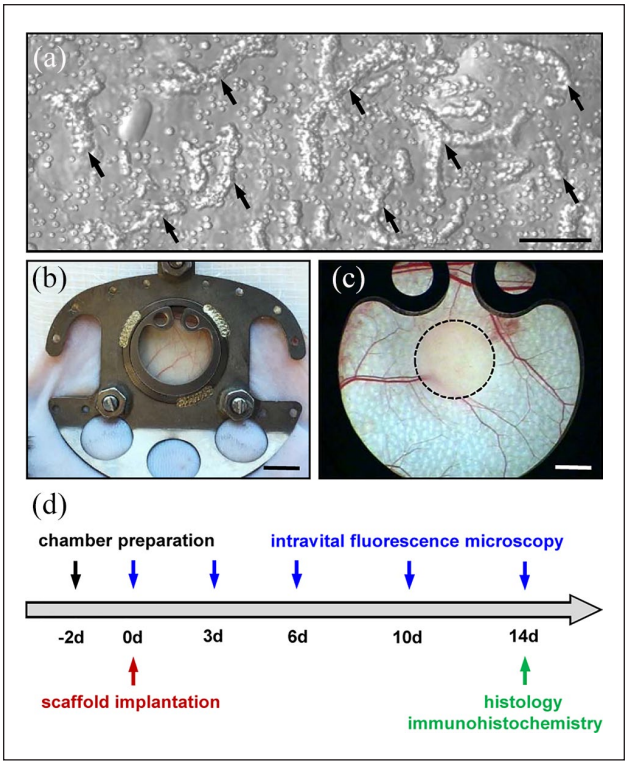

Figure 1. Model and experimental study design: (a) Brightfield microscopy of ad-MVFs (arrows) directly after enzymatic isolation from the epididymal fat pads of a GFP$^+$ donor mouse. Scale bar: 80 µm. (b) Dorsal skinfold chamber on the back of a C57BL/6 mouse. Scale bar: 5 mm. (c) Stereomicroscopy of the observation window of a dorsal skinfold chamber after the implantation of an ad-MVF-seeded collagen–glycosaminoglycan scaffold (borders marked by a broken line). Scale bar: 1.5 mm. (d) Time scheme of the dorsal skinfold chamber experiments. Two days after the chamber preparation, ad-MVF-seeded scaffolds were implanted and repetitively analyzed by means of intravital fluorescence microscopy on days 0, 3, 6, 10, and 14. Thereafter, the dorsal skinfold chamber tissue with the implants was excised and additionally analyzed by histology and immunohistochemistry.

Materials and methods

Animals

Ad-MVFs were isolated from the epididymal fat pads of male C57BL/6 wild-type mice or C57BL/6-TgN(ACTB-EGFP)1Osb/J mice (age: 6–12 months; body weight: >30 g; Institute for Clinical & Experimental Surgery, Saarland University, Homburg/Saar, Germany), which ubiquitously express green fluorescent protein (GFP).[17] Male GFP$^-$ C57BL/6 wild-type mice (age: 5–7 months; body weight: 24–26 g) with implanted dorsal skinfold chambers served as recipient animals. The mice were housed in the animal facility of the Institute for Clinical & Experimental Surgery (Saarland University, Homburg/Saar, Germany) with free access to tap water and standard pellet food (Altromin, Lage, Germany).

This study was approved by the local governmental animal protection committee (Landesamt für Verbraucherschutz, Saarbrücken; permission number: 29/2014) and conducted in accordance with the Directive 2010/63/EU and the NIH Guidelines for the Care and Use of Laboratory Animals (NIH Publication #85-23 Rev. 1985).

Isolation and cultivation of ad-MVFs

For the isolation of ad-MVFs (Figure 1(a)), donor mice were anesthetized by an intraperitoneal injection of ketamine (75 mg kg^{-1} of body weight, Ursotamin®; Serumwerke Bernburg, Bernburg, Germany) and xylazine (25 mg kg^{-1} of body weight, Rompun®; Bayer, Leverkusen, Germany). The isolation was performed as previously described in detail.[4]

Briefly, both epididymal fat pads were harvested and washed in phosphate-buffered saline (PBS). Subsequently, they were mechanically minced with a micro-scissors and enzymatically digested in collagenase NB4G (0.5 U mL^{-1}; Serva, Heidelberg, Germany) for 10 min under slow stirring at 37°C in a humidified atmosphere with 5% CO_2. The collagenase was then neutralized with PBS containing 20% fetal calf serum (FCS). The resulting ad-MVF suspension was incubated three to five times for 5 min at 37°C, and the fat supernatants were removed. After filtration through a 500-µm mesh, the ad-MVFs were enriched to a final pellet by centrifugation at 120 × *g* for 5 min.

The isolated ad-MVFs were divided into three equal parts and cultivated for 24 h under humidified conditions in 1% agarose–coated 24-well plates filled with 4°C UW solution (Belzer UW® Cold Storage Solution, Bridge to Life Ltd., Columbia, SC, USA). Recently, we could demonstrate that these conditions are suitable for the xeno-free cultivation of ad-MVFs in accordance with good manufacturing practices.[11] The UW solution was supplemented with vehicle (PBS), 1-µM IGF-1 (R&D Systems, Wiesbaden, Germany), or a combination of 1-µM IGF-1 and 0.5-µg mL^{-1} IGFbp4 (R&D Systems). After cultivation, the ad-MVFs were washed in PBS and analyzed by means of different in vitro and in vivo approaches.

Flow cytometry

The cellular composition of cultivated ad-MVFs was assessed by means of flow cytometry. For this purpose, the ad-MVFs were digested in Accutase® (BioLegend, Fell, Germany) for 30 min at 37°C into single cells. Subsequently, the cellular expression of the endothelial cell marker CD31, the pericyte marker α-smooth muscle actin (α-SMA), and the stromal/stem cell surface markers CD73 and CD117 was measured with phycoerythrin (PE)- or fluorescein isothiocyanate (FITC)-labeled antibodies (BD Pharmingen, Heidelberg, Germany) by means of a FACScan (BD Biosciences, Heidelberg, Germany) and the software package CellQuest Pro (BD Biosciences). Isotype-identical IgG-PE and IgG-FITC (BD Pharmingen) served as controls.

Western blot analysis

To study the expression of vascular endothelial growth factor (VEGF), VEGF receptor-2 (VEGFR-2) and matrix metalloproteinase (MMP)-2 of ad-MVFs and cultivated ad-MVFs were transferred into lysis buffer, shock frozen in liquid nitrogen, and stored at −80°C. For protein extraction, the ad-MVFs were lysed by homogenization with additional protease inhibitors (0.5-mM phenylmethylsulfonyl fluoride, 1:75 v/v Protease Inhibitor Cocktail, 1:100 v/v Phosphatase Inhibitor Cocktail 2; Sigma-Aldrich, Taufkirchen, Germany). The lysates were then centrifuged at 4°C and 16,000 × *g* for 30 min, and supernatants were saved as whole protein extracts. Protein concentrations were analyzed by means of the Lowry method. Subsequently, 30-µg protein per lane was separated on 10% sodium dodecyl sulfate–polyacrylamide gels and transferred to a polyvinylidene difluoride membrane (Bio-Rad Laboratories, München, Germany). The membranes were incubated over night at 4°C and for additional 3 h at room temperature with primary antibodies against VEGF (1:50; Santa Cruz Biotechnology, Heidelberg, Germany), VEGFR-2 (1:300; Cell Signaling Technology, Frankfurt, Germany), and MMP-2 (1:100; Santa Cruz Biotechnology). Corresponding horseradish peroxidase–conjugated secondary antibodies (1:1000; R&D Systems) were attached at room temperature for 1.5 h. Protein expression was visualized with enhanced chemiluminescence (ECL Western Blotting Analysis System, GE Healthcare) and analyzed with an ECL ChemoCam Imager (Chemostar and LabImage 1D software; Intas Science Imaging Instruments, Göttingen, Germany). The data were normalized to β-actin signals (mouse monoclonal anti-β-actin antibody, 1:5000; Sigma-Aldrich) to correct unequal loading.

Scaffold preparation and seeding

For the in vivo analyses, the cultivated ad-MVFs were seeded onto clinically available collagen–glycosaminoglycan scaffolds (Integra®; Integra GmbH, Ratingen, Germany) with a diameter of 3 mm. Seeding was performed as previously described in detail.[11]

Dorsal skinfold chamber model and intravital fluorescence microscopy

The in vivo vascularization of ad-MVF-seeded scaffolds was analyzed by means of intravital fluorescence microscopy directly (day 0) as well as on days 3, 6, 10, and 14 after implantation into dorsal skinfold chambers of GFP$^-$ C57BL/6 recipient mice (Figure 1(b)–(d)), as described previously in detail.[10] Before each microscopy, the anesthetized mice received a retrobulbary injection of 0.1-mL 5% FITC-labeled dextran 150,000 (Sigma-Aldrich) for contrast enhancement by intravascular plasma staining. The microscopic images were analyzed with the computer-assisted offline analysis system CapImage (Zeintl, Heidelberg, Germany). The vascularization of the implants was assessed in eight regions of interest (ROIs). Perfused ROIs (in % of all ROIs) were defined as areas containing either newly developed red blood cell (RBC)-perfused microvessels or reperfused GFP$^+$ ad-MVFs. In addition, we measured the functional microvessel density, that is, the length of all RBC-perfused microvessels per ROI given in cm cm^{-2}, as well as the diameter (d; given in µm) and the centerline RBC velocity (v; given in µm s^{-1}) of 30 randomly selected perfused microvessels within the implants.

The wall shear rate (y; given in s^{-1}) of these vessels was then calculated according to $y = 8 \times v/d$.

Histology and immunohistochemistry

Histological and immunohistochemical analyses were performed on formalin-fixed specimens of cultivated ad-MVFs, which were embedded in 200-µL fibrin clots (Hepato-Prest®; Diagnostica Stago, Asnières-sur-Seine, France) and dorsal skinfold preparations with ad-MVF-seeded implants. For this purpose, they were embedded in paraffin and cut into 3-µm-thick sections. Hematoxylin and eosin (HE) staining was performed according to standard procedures.

To study the presence and expression levels of IGF-1 receptor (IGF-1R) within ad-MVFs, sections of fibrin-embedded ad-MVFs were co-stained with an antibody against the endothelial cell marker CD31 (1:100; Dianova, Hamburg, Germany) in combination with an antibody against IGF-1R (1:50; Abcam, Cambridge, UK). A goat anti-rat IgG antibody (1:200; Life Technologies, Eugene, OR, USA) and a goat anti-rabbit Alexa555 IgG antibody (1:200; Thermo Fisher Scientific GmbH, Dreieich, Germany) served as secondary antibodies. To merge the images, cell nuclei on each section were stained with Hoechst 33342 (2 µg mL^{-1}; Sigma-Aldrich). The sections were examined under a BX60 microscope (Olympus, Hamburg, Germany).

For the immunohistochemical analysis of cell viability and proliferation, sections of fibrin-embedded ad-MVFs were co-stained with an antibody against CD31 in combination with an antibody against the apoptosis marker cleaved caspase (Casp)-3 or the proliferation marker Ki67, as described previously in detail.[10] The sections were quantitatively analyzed for the assessment of the fractions of $CD31^+/Casp\text{-}3^+$ and $CD31^+/Ki67^+$ endothelial cells (given in %) as well as $CD31^-/Casp\text{-}3^+$ and $CD31^-/Ki67^+$ perivascular cells (given in %) in randomly selected fibrin-embedded ad-MVFs, including at least 200 endothelial and perivascular cells per sample.

In addition, sections of dorsal skinfold preparations with ad-MVF-seeded implants were co-stained with an antibody against CD31 and GFP, as described previously in detail.[10] These sections were used to assess the density of all $CD31^+$ microvessels (given in mm^{-2}) and the fraction of $CD31^+/GFP^+$ microvessels of all $CD31^+$ microvessels (given in %) in the center and the border zones of the implants.

Experimental protocol

For in vitro analyses, ad-MVFs were harvested from 54 C57BL/6 wild-type donor mice. After cultivation, their cellular composition and protein expression were analyzed by flow cytometry (n = 3 for each group) and Western blotting (n = 4 for each group). Additional ad-MVFs were used for the immunohistochemical analysis of IGF-1R expression, cell viability, and proliferation (n = 4 for each group).

For in vivo analyses, ad-MVFs were harvested from 37 GFP^+ donor mice. After their cultivation, they were seeded onto scaffolds, which were implanted into the dorsal skinfold chambers of 24 GFP^- recipient mice (vehicle: n = 8; IGF-1: n = 8; IGF-1 + IGFbp4: n = 8) for repetitive intravital fluorescence microscopy. Finally, the animals were sacrificed with an overdose of anesthetics and the implants were further processed for histological and immunohistochemical analyses.

Table 1. Ad-MVF cells expressing CD31, α-SMA, CD73, and CD117 (% of all cells), as assessed by flow cytometry.

	CD31	α-SMA	CD73	CD117
Vehicle	25.6 ± 2.6	9.8 ± 1.5	16.3 ± 1.7	20.4 ± 1.4
IGF-1	30.2 ± 2.0	13.2 ± 3.2	20.1 ± 0.5	25.0 ± 1.8
IGF-1 + IGFbp4	30.0 ± 1.0	13.6 ± 1.7	21.6 ± 0.6	22.8 ± 2.4

Ad-MVF: adipose tissue–derived microvascular fragment; UW: University of Wisconsin; IGF-1: insulin-like growth factor 1; IGFbp4: insulin-like growth factor–binding protein 4; SMA: smooth muscle actin; SEM: standard error of the mean.
Mean ± SEM.
The ad-MVFs were cultivated for 24 h in 4°C UW solution supplemented with vehicle (n = 3), IGF-1 (n = 3), or a combination of IGF-1 and IGFbp4 (n = 3).

Statistical analysis

All data were tested for normal distribution and equal variance. In case of parametric distribution of the data, differences between the three groups were analyzed by analysis of variance (ANOVA) followed by the Student–Newman–Keuls post hoc test. In case of non-parametric distribution of the data, differences were assessed by ANOVA on ranks followed by Dunn's test (SigmaPlot 11.0; Jandel Corporation, San Rafael, CA, USA). All values are given as mean ± standard error of the mean (SEM). Statistical significance was accepted for a value of $p < 0.05$.

Results

Cellular composition of ad-MVFs

We first performed flow cytometric analyses of ad-MVFs directly after their cultivation in 4°C UW solution, which was supplemented with vehicle, IGF-1, or a combination of IGF-1 and IGFbp4. These analyses revealed that the different supplements did not affect the cellular composition of the vessel segments. In all the three groups, we detected ~ 26–30% $CD31^+$ endothelial cells and ~ 10–14% α-SMA^+ pericytes (Table 1). In addition, the ad-MVFs also contained ~ 16–25% cells, which were positive for the stromal/stem cell surface markers CD73 or CD117 (Table 1).

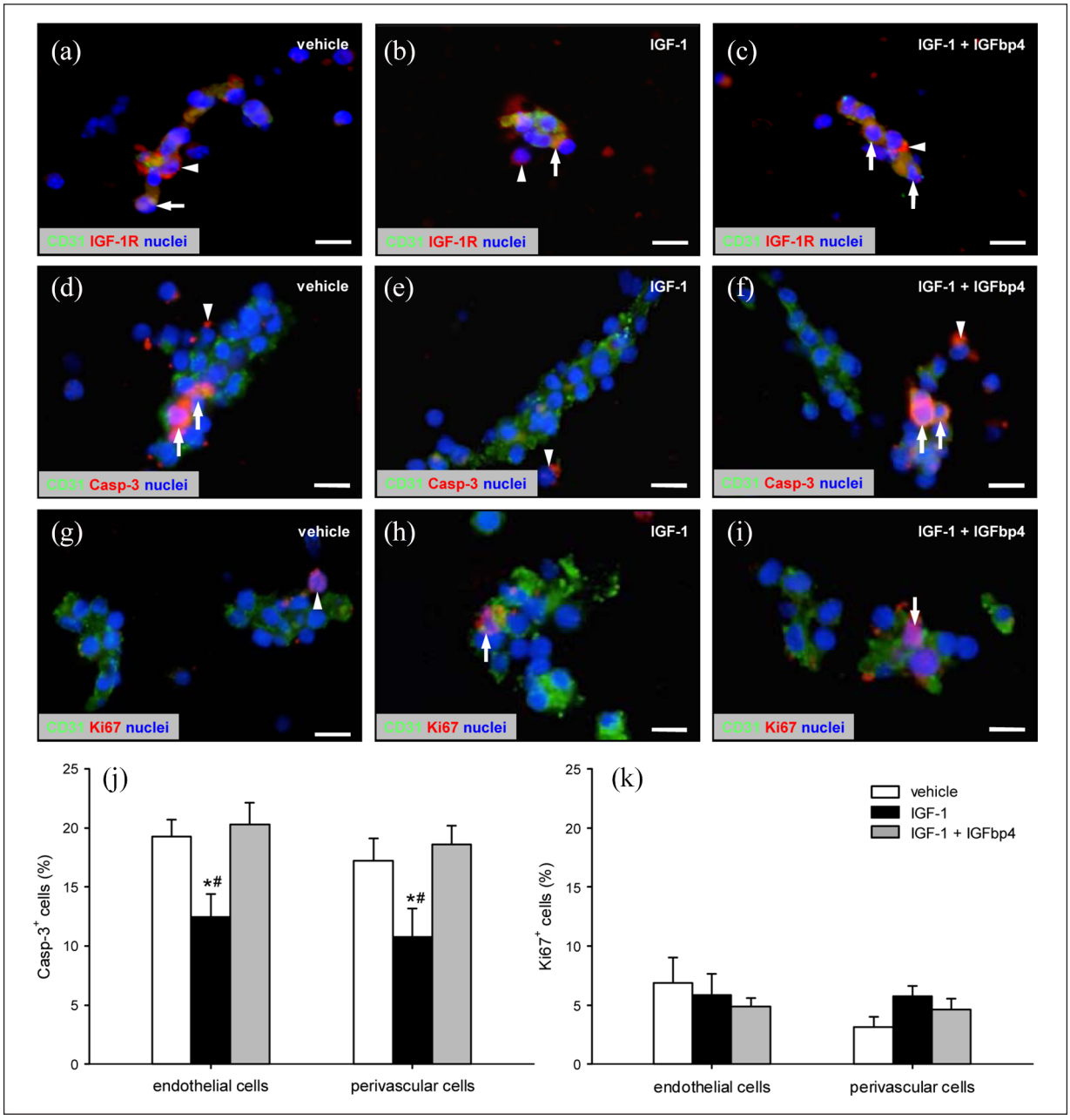

Figure 2. IGF-1R expression, viability, and proliferative activity of ad-MVFs: (a–i) Fluorescence microscopy of fibrin-embedded ad-MVFs, which were cultivated for 24 h in 4°C UW solution supplemented with vehicle (a, d, g), IGF-1 (b, e, h), or a combination of IGF-1 and IGFbp4 (c, f, i). Staining was performed with Hoechst 33342 (a–i, blue) for the detection of cell nuclei and an antibody against CD31 (a–i; green) for the identification of endothelial cells in combination with an antibody against IGF-1R (a–c, red), an antibody against Casp-3 (d–f; red) for the labeling of apoptotic cells, or an antibody against Ki67 (g–i; red) for the labeling of proliferating cells. Arrows = marker-positive endothelial cells, arrowheads = marker-positive perivascular cells. Scale bars: 11 µm. (j) Casp-3$^+$ apoptotic (%) and (k) Ki67$^+$ proliferating (%) cells within ad-MVFs, which were cultivated for 24 h in 4°C UW solution supplemented with vehicle (white bars, n = 4), IGF-1 (black bars, n = 4), or a combination of IGF-1 and IGFbp4 (gray bars, n = 4). Mean ± SEM; $^*p < 0.05$ vs vehicle; $^\#p < 0.05$ vs IGF-1 + IGFbp4.

IGF-1R expression, viability, and proliferative activity of ad-MVFs

In a second set of experiments, we analyzed the expression of IGF-1R as well as the viability and proliferative activity of endothelial cells and surrounding perivascular cells within cultivated, fibrin-embedded ad-MVFs by means of immunohistochemistry. We found that IGF-1R is strongly expressed on both endothelial and perivascular cells of ad-MVFs (Figure 2(a)–(c)). This confirms the findings of a previous study reporting the expression of IGF-1R in the SVF of adipose tissue but not on adipocytes.[16]

Ad-MVFs cultivated in the vehicle-supplemented UW solution exhibited ~ 19% endothelial cells and ~ 17% perivascular cells, which stained positive for the apoptosis marker Casp-3 (Figure 2(d) and (j)). This high apoptosis rate was significantly reduced, when ad-MVFs were cultivated in the IGF-1-supplemented UW solution (Figure 2(e) and (j)). Addition of IGFbp4, in turn, completely reversed this positive effect of IGF-1 on cell viability (Figure 2(f) and (j)). Moreover, we detected ~ 5–7% Ki67$^+$ endothelial cells and ~ 3–6% Ki67$^+$ perivascular cells without significant differences between the groups (Figure 2(g)–(i) and (k)). This indicates that the different supplements had no effect on the proliferative activity of ad-MVFs.

Angiogenic activation of ad-MVFs

To assess the angiogenic activation of cultivated ad-MVFs, we next measured the expression of the pro-angiogenic factors VEGF/VEGFR-2 and MMP-2 by means of Western blot. Cultivation of ad-MVFs in the UW solution supplemented with IGF-1 or IGF-1 in combination with IGFbp4 markedly increased their expression of VEGF and VEGFR-2 when compared to vehicle-treated controls (Figure 3). In addition, we detected a higher expression of MMP-2, which, however, was not proven to be significant (Figure 3).

In vivo vascularization capacity of ad-MVFs

Finally, we seeded cultivated ad-MVFs onto collagen–glycosaminoglycan scaffolds, which were implanted into dorsal skinfold chambers of recipient mice to study their vascularization using repetitive intravital fluorescence microscopy. By means of this approach, we could demonstrate that cultivation of ad-MVFs in IGF-1-supplemented UW solution accelerates and improves their in vivo vascularization capacity. In fact, scaffolds seeded with these ad-MVFs exhibited a significantly higher number of blood-perfused ROIs already on day 3 after implantation when compared to those seeded with vehicle-treated controls (Figure 4(a), (b) and (g)). In addition, they finally contained newly formed microvascular networks with a significantly higher functional microvessel density on day 10 and 14 (Figure 4(d), (e) and (h)). This was associated with improved microhemodynamic parameters. Individual microvessels within the scaffolds seeded with IGF-1-stimulated ad-MVFs presented with significantly reduced diameters on day 10 and 14 when compared to those seeded with vehicle-exposed ad-MVFs, which is a typical sign for enhanced vessel maturation and remodeling (Table 2). In addition, these vessels also exhibited higher centerline RBC velocities and wall shear rates (Table 2). All these positive effects of IGF-1 stimulation were completely reversed by addition of IGFbp4 to the UW solution during ad-MVF cultivation (Figure 4(c), (f)–(h) and Table 2).

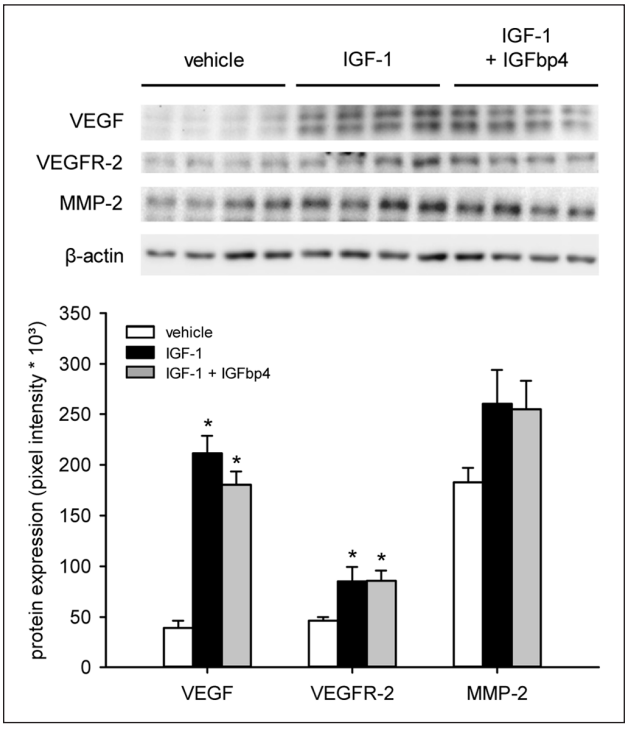

Figure 3. Angiogenic activation of ad-MVFs. Western blot analysis of the expression (pixel intensity × 10³) of VEGF, VEGFR-2, and MMP-2 within ad-MVFs, which were cultivated for 24 h in 4°C UW solution supplemented with vehicle (white bars, n = 4), IGF-1 (black bars, n = 4), or a combination of IGF-1 and IGFbp4 (gray bars, n = 4). The data were normalized to β-actin signals to correct unequal loading.
Mean ± SEM; $^*p < 0.05$ vs vehicle.

At the end of the in vivo experiments, we additionally analyzed implanted ad-MVF-seeded scaffolds by means of histology and immunohistochemistry. In line with our intravital fluorescent microscopic results, we found that scaffolds seeded with IGF-1-stimulated ad-MVFs were better incorporated at the implantation site when compared to the other two groups, as indicated by a more pronounced invasion of granulation tissue at the margins and the center of the implants (Figure 5(a)–(i)). Moreover, we detected a higher density of CD31$^+$ microvessels within their center and the border zones (Figure 5(j), (k) and (n)). In contrast, there were no significant differences in the fraction of CD31$^+$/GFP$^+$ microvessels (Figure 5(k)–(m) and (o)). The analyzed border and center zones of the implants of all three groups exhibited fractions higher than 80% CD31$^+$/GFP$^+$ microvessels (Figure 5(o)).

Discussion

Ad-MVFs represent versatile vascularization units for different applications in the field of tissue engineering

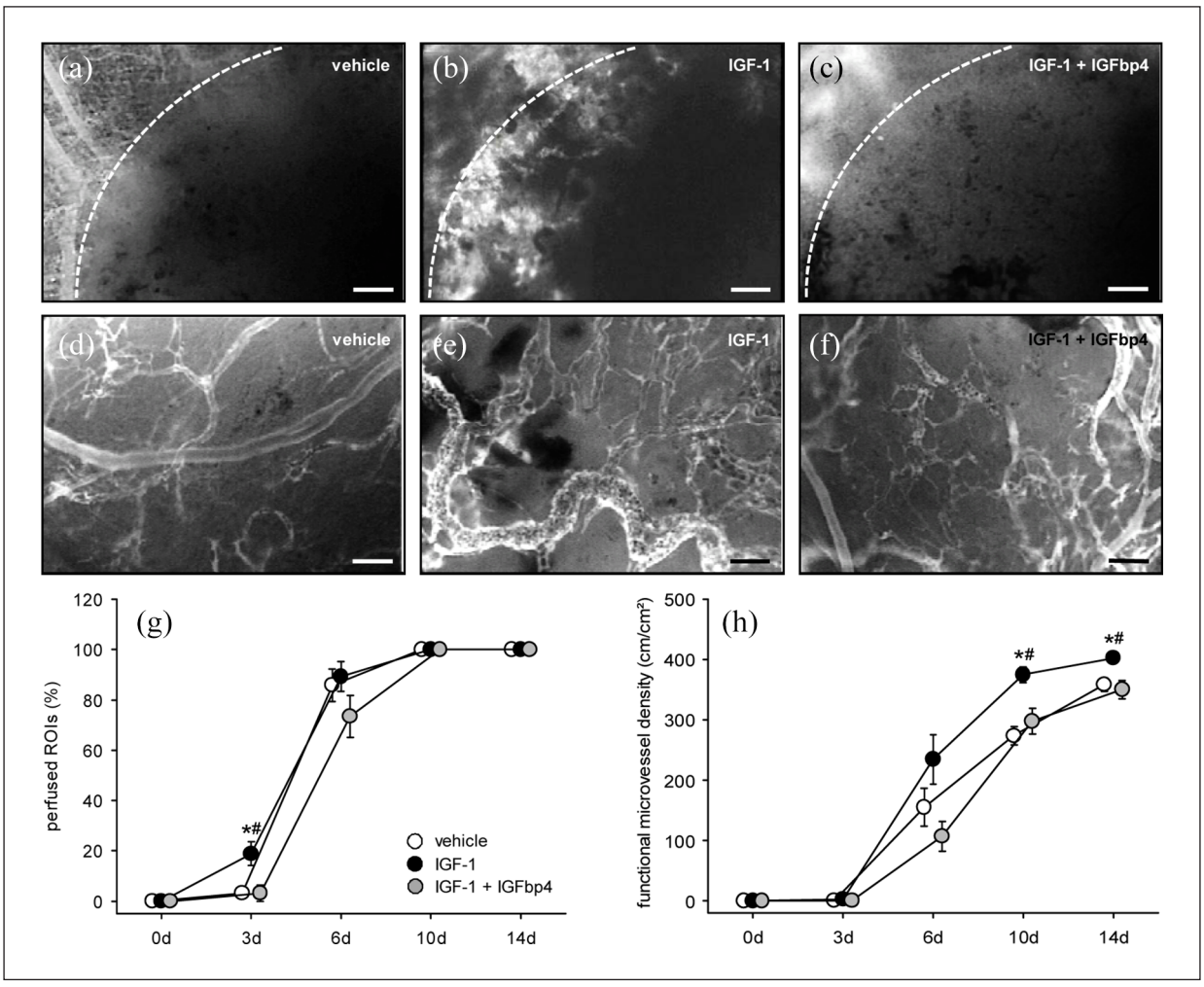

Figure 4. In vivo vascularization capacity of ad-MVFs: (a–f): Intravital fluorescence microscopy (blue light epi-illumination with contrast enhancement by 5% FITC–labeled dextran 150,000 i.v.) of ad-MVF-seeded collagen–glycosaminoglycan scaffolds (borders marked by broken lines in (a–c)) on day 3 (a–c) and 14 (d–f) after implantation into the dorsal skinfold chamber of C57BL/6 mice. The ad-MVFs were cultivated for 24 h in 4°C UW solution supplemented with vehicle (a, d), IGF-1 (b, e), or a combination of IGF-1 and IGFbp4 (c, f). Scale bars: (a–c) = 170 µm and (d–f) = 70 µm. (g) Perfused ROIs (%) and (h) functional microvessel density ($cm\,cm^{-2}$) of ad-MVF-seeded collagen–glycosaminoglycan scaffolds directly (0d) as well as 3, 6, 10, and 14 days after implantation into dorsal skinfold chambers, as assessed by intravital fluorescence microscopy. The ad-MVFs were cultivated for 24 h in 4°C UW solution supplemented with vehicle (white circles, n = 8), IGF-1 (black circles, n = 8), or a combination of IGF-1 and IGFbp4 (gray circles, n = 8). Mean ± SEM; $^{*}p < 0.05$ vs vehicle; $^{\#}p < 0.05$ vs IGF-1 + IGFbp4.

and regenerative medicine. In previous studies, they have been used to establish a sufficient blood supply to surgical flaps,[18,19] epicardial patches,[20] muscle and bone defects[21,22] as well as dermal skin substitutes.[7] Although they already exhibit the unique ability to rapidly reassemble into new blood-perfused microvascular networks, we have recently shown that their vascularization capacity can be further improved during short-term 24-h cultivation prior to their in vivo use.[12] In the present study, we now demonstrate that this is achieved by adding IGF-1 as a culture supplement.

Our novel approach is based on the finding that the angiogenic activity of blood vessels in adipose tissue is typically determined by metabolic signals.[16] Indeed, increased insulin levels in the course of high-fat diet promote the vascular sprouting of adipose tissue, which is mediated by the upregulation of IGF-1 and downregulation of IGFbp4.[16] In line with this view, we herein found that stimulation of isolated ad-MVFs with IGF-1 does not affect their cellular composition but markedly enhances their expression of VEGF/VEGFR-2 and MMP-2 when compared to vehicle-treated controls. Additional exposure to IGFbp4 did not reverse this pro-angiogenic effect, indicating that IGF-1 induces the expression of the analyzed factors independently of the interaction with IGFbp4. Another possible explanation for this unexpected observation may be the inefficiency of IGFbp4 to interact with the IGF-1R in the present

Table 2. Diameter (μm), centerline RBC velocity (μm s^{-1}), and wall shear rate (s^{-1}) of individual microvessels within ad-MVF-seeded collagen–glycosaminoglycan scaffolds on day 3, 6, 10, and 14 after implantation into dorsal skinfold chambers, as assessed by intravital fluorescence microscopy.

	Day 3	Day 6	Day 10	Day 14
Diameter (μm)				
Vehicle	55.5 ± 9.8	21.2 ± 0.8	15.7 ± 0.8	12.9 ± 0.5
IGF-1	32.1 ± 6.7	21.8 ± 1.5	12.5 ± 0.5*#	10.4 ± 0.4*#
IGF-1 + IGFbp4	39.6 ± 4.7	24.1 ± 1.8	15.0 ± 0.6	13.2 ± 0.7
Centerline RBC velocity (μm s^{-1})				
Vehicle	25.0 ± 3.0	194.4 ± 28.1	284.9 ± 33.5	360.1 ± 21.9
IGF-1	39.5 ± 9.8	185.1 ± 28.9	385.2 ± 30.3*#	451.3 ± 13.2*#
IGF-1 + IGFbp4	13.6 ± 11.1	96.7 ± 16.6	243.0 ± 34.7	341.1 ± 23.4
Wall shear rate (s^{-1})				
Vehicle	5.0 ± 2.3	86.7 ± 12.3	178.8 ± 23.9	259.0 ± 17.0
IGF-1	26.6 ± 14.4	77.7 ± 13.4	276.9 ± 17.4*#	402.8 ± 21.2*#
IGF-1 + IGFbp4	2.9 ± 2.4	39.0 ± 7.7	165.1 ± 30.0	255.1 ± 24.5

Ad-MVF: adipose tissue–derived microvascular fragments; UW: University of Wisconsin; IGF-1: insulin-like growth factor 1; IGFbp4: insulin-like growth factor–binding protein 4; RBC: red blood cell; SEM: standard error of the mean.
The ad-MVFs were cultivated for 24 h in 4°C UW solution supplemented with vehicle (n = 8), IGF-1 (n = 8), or a combination of IGF-1 and IGFbp4 (n = 8).
Mean ± SEM; *$p < 0.05$ vs vehicle; #$p < 0.05$ vs IGF-1 + IGFbp4.

experimental setting due to wrong doses of IGFbp4 and IGF-1 or a lack of IGFbp4 action time because both compounds were applied simultaneously. However, we planned our experiments according to the protocols and results of previous studies focusing on the interaction of IGFbp4 and IGF-1. In these studies, the dose of 0.5 μg mL^{-1} IGFbp4 has been shown to potently inhibit IGF-1-induced angiogenesis.[16,23] For this purpose, IGFbp4 and doses of IGF-1 up to 10 μM were also applied at the same time to different angiogenesis assays. Moreover, we could demonstrate that 1-μM IGF-1 effectively protects the endothelial and perivascular cells of ad-MVFs from apoptotic cell death during cultivation, which is completely reversed by co-exposure with 0.5-μg mL^{-1}-IGFbp4. The latter finding confirms previous studies reporting on anti-apoptotic mechanisms of the growth factor.[24,25] In endothelial cells, these mechanisms particularly involve the preservation of the mitochondrial membrane potential and retention of cytochrome-c as well as a reduction of Casp-3 activity.[25]

It is also well known that IGF-1 promotes the proliferation of endothelial cells and perivascular smooth muscle cells via activation of the PI3K (phosphoinositide 3-kinase)/Akt pathway.[26,27] However, our immunohistochemical analyses did not reveal any differences in the fraction of proliferating $Ki67^+$ cells within vehicle-, IGF-1-, and IGF-1/IGFbp4-exposed ad-MVFs. This is most probably due to the fact that the ad-MVFs were cultivated under hypothermic conditions, which have been shown to suppress cell proliferation.[28,29] We chose these conditions because we wanted to use the UW solution for our experiments, which would also be suitable to cultivate ad-MVFs under clinical conditions in accordance with good manufacturing practices. Recently, we found that for this purpose, it is more favorable to cultivate ad-MVFs at a low temperature of 4°C because this prevents their aggregation into larger agglomerates and, thus, facilitates their subsequent homogeneous seeding onto collagen–glycosaminoglycan scaffolds.[11]

The in vivo vascularization of ad-MVF-seeded scaffolds was assessed in the dorsal skinfold chamber by means of intravital fluorescence microscopy. In line with our in vitro results, we found that scaffolds, which were seeded with IGF-1-stimulated ad-MVFs, exhibited a faster vascularization, as indicated by a significantly higher number of perfused ROIs on day 3 after implantation when compared to the other two groups. A more rapid onset of blood perfusion in newly developing microvascular networks is associated with an accelerated vascular remodeling process over time.[30] Accordingly, we detected a more pronounced decrease of the diameter and increase of the centerline RBC velocity of individual microvessels in scaffolds of the IGF-1 group at later observation time points. These improved microhemodynamic conditions also resulted in higher wall shear rates, which are known to promote vascular sprouting.[31] Hence, it may be assumed that this mechanism crucially contributed to the formation of microvascular networks, which finally exhibited a higher functional microvessel density in scaffolds seeded with IGF-1-stimulated ad-MVFs when compared to those seeded with vehicle- or IGF-1/IGFbp4-exposed vessel segments.

Finally, we analyzed the implanted scaffolds on day 14 by means of histology and immunohistochemistry. Of interest, we detected a strong invasion of granulation

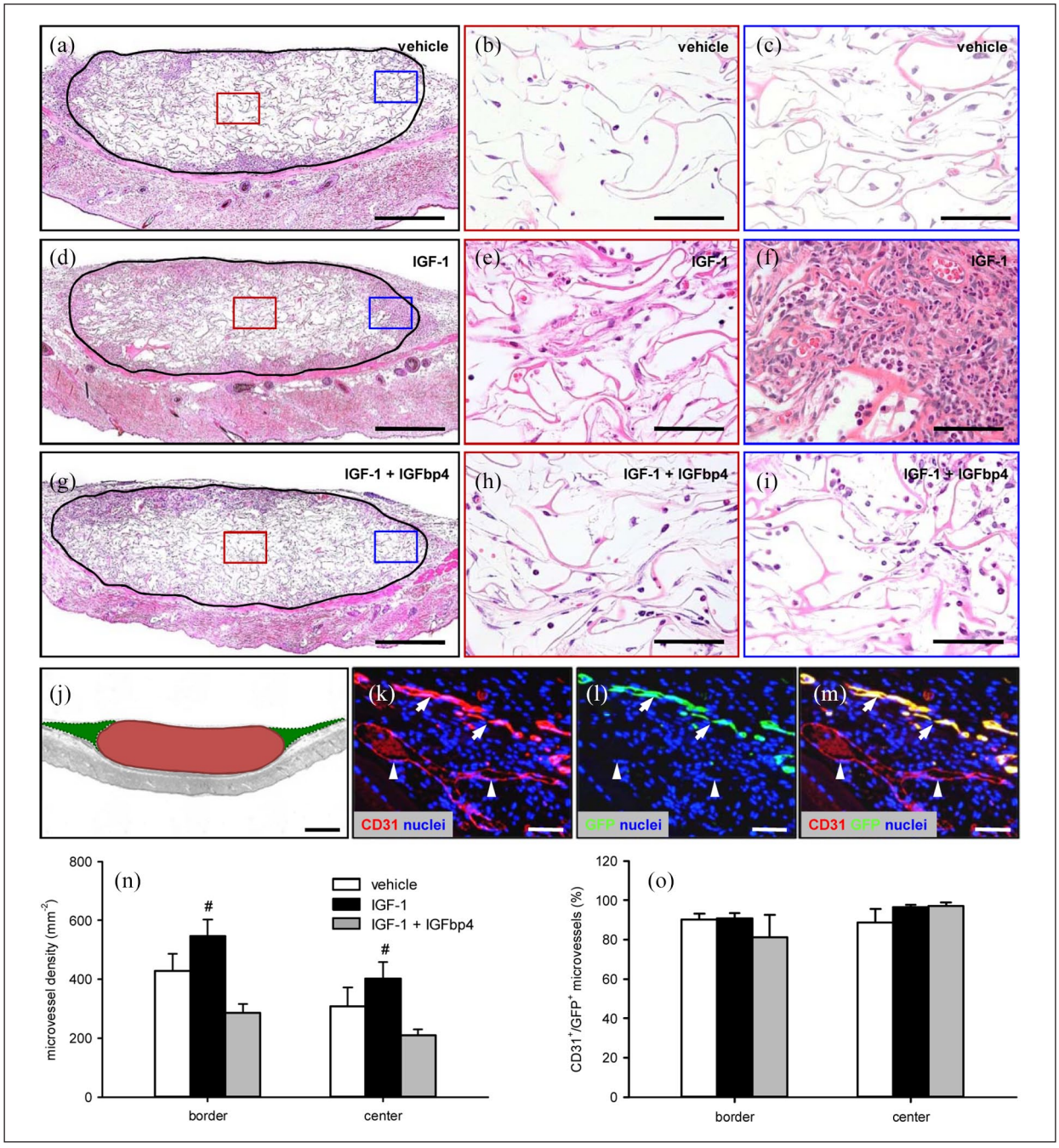

Figure 5. Final vascularization and incorporation of ad-MVF-seeded scaffolds: (a–i): HE-stained sections of ad-MVF-seeded collagen–glycosaminoglycan scaffolds (borders marked by closed line; b, e, h = red inserts in a, d, g; c, f, i = blue inserts in a, d, g) on day 14 after implantation into the dorsal skinfold chamber of C57BL/6 mice. The ad-MVFs were cultivated for 24 h in 4°C UW solution supplemented with vehicle (a–c), IGF-1 (d–f), or a combination of IGF-1 and IGFbp4 (g–i). Scale bars: a, d, g = 380 µm and b, c, e, f, h, i = 60 µm. (j): Scheme displaying the different areas, which were used for the immunohistochemical analyses (red = implanted scaffold (center) and green = surrounding host tissue (border)). Scale bar = 620 µm. (k–m): Representative images of immunohistochemically stained microvessels in the center of an ad-MVF-seeded collagen–glycosaminoglycan scaffold on day 14 after implantation into the dorsal skinfold chamber of a C57BL/6 mouse. Staining was performed with Hoechst 33342 to identify cell nuclei (k–m, blue), an antibody against CD31 for the detection of endothelial cells (k, red) and an antibody against GFP (l, green). (m) The merge of (k) and (l). Arrows = $CD31^+/GFP^+$ microvessels and arrowheads = $CD31^+/GFP^-$ microvessels. Scale bars: 70 µm. (n) Microvessel density (mm^{-2}) and (o) $CD31^+/GFP^+$ microvessels (%) in the center and border zones of ad-MVF-seeded collagen–glycosaminoglycan scaffolds 14 days after implantation into the dorsal skinfold chamber, as assessed by immunohistochemical analysis. The ad-MVFs were cultivated for 24 h in 4°C UW solution supplemented with vehicle (white bars, n = 8), IGF-1 (black bars, n = 8), or a combination of IGF-1 and IGFbp4 (gray bars, n = 8). Mean ± SEM; $^{\#}p < 0.05$ vs IGF-1 + IGFbp4.

tissue into scaffolds seeded with IGF-1-stimulated ad-MVFs. This observation can be interpreted as a stronger incorporation of the implants at the end of the observation period due to their improved vascularization. In fact, these scaffolds also presented with the highest density of $CD31^+$ microvessels when compared to the other two groups. More detailed analyses further revealed that the fraction of $CD31^+/GFP^+$ microvessels was comparably high (>80%) in the border and center zones of the scaffolds of all the three groups. Importantly, these immunohistochemical findings indicate that in all the three groups, the vascularization of the implants was mainly driven by the seeded GFP^+ ad-MVFs. Moreover, they show that the absolute number of $CD31^+/GFP^+$ microvessels was significantly higher in the IGF-1 group, while the fraction of $CD31^+/GFP^+$ microvessels did not differ between the groups. This is most probably due to the fact that IGF-1 not only improved the viability of GFP^+ ad-MVFs within the scaffolds and stimulated their outgrowth into the surrounding host tissue but also simultaneously promoted to the same extent angiogenesis of GFP^- host microvessels within the scaffolds' border zones and their angiogenic ingrowth into the implants.

Conclusion

We could demonstrate that IGF-1 improves the viability, angiogenic activity, and in vivo network-forming capacity of ad-MVFs. Accordingly, exposure of isolated ad-MVFs to this growth factor during short-term cultivation may represent a promising approach to improve their vascularization properties prior to their retransfer into patients during multi-step surgical procedures.

Acknowledgements

We are grateful for the excellent technical assistance of Janine Becker, Caroline Bickelmann, Ruth M. Nickels, and Julia Parakenings (Institute for Clinical & Experimental Surgery, Saarland University, Homburg/Saar, Germany).

Availability of data and materials

All data can be obtained in this manuscript.

Declaration of conflicting interest

The author(s) declared no potential conflicts of interest with respect to the research, authorship, and/or publication of this article.

Ethical approval

This study was approved by the local governmental animal protection committee (Landesamt für Verbraucherschutz, Saarbrücken; permission number: 29/2014) and conducted in accordance with the Directive 2010/63/EU and the NIH Guidelines for the Care and Use of Laboratory Animals (NIH Publication #85-23 Rev. 1985).

Funding

The author(s) disclosed receipt of the following financial support for the research, authorship, and/or publication of this article: This study was funded by a grant of the Deutsche Forschungsgemeinschaft (DFG: German Research Foundation)—LA 2682/7–1.

ORCID iD

Matthias W Laschke https://orcid.org/0000-0002-7847-8456

References

1. Laschke MW and Menger MD. Prevascularization in tissue engineering: current concepts and future directions. *Biotechnol Adv* 2016; 34(2): 112–121.
2. Rouwkema J and Khademhosseini A. Vascularization and angiogenesis in tissue engineering: beyond creating static networks. *Trends Biotechnol* 2016; 34(9): 733–745.
3. Laschke MW and Menger MD. Adipose tissue-derived microvascular fragments: natural vascularization units for regenerative medicine. *Trends Biotechnol* 2015; 33(8): 442–448.
4. Frueh FS, Später T, Scheuer C, et al. Isolation of murine adipose tissue-derived microvascular fragments as vascularization units for tissue engineering. *J Vis Exp* 2017; 122: 55721.
5. Muller AM, Mehrkens A, Schafer DJ, et al. Towards an intraoperative engineering of osteogenic and vasculogenic grafts from the stromal vascular fraction of human adipose tissue. *Eur Cell Mater* 2010; 19: 127–135.
6. Farré-Guasch E, Bravenboer N, Helder MN, et al. Blood vessel formation and bone regeneration potential of the stromal vascular fraction seeded on a calcium phosphate scaffold in the human maxillary sinus floor elevation model. *Materials (Basel)* 2018; 11(1): 161.
7. Frueh FS, Später T, Lindenblatt N, et al. Adipose tissue-derived microvascular fragments improve vascularization, lymphangiogenesis, and integration of dermal skin substitutes. *J Invest Dermatol* 2017; 137(1): 217–227.
8. Später T, Frueh FS, Nickels RM, et al. Prevascularization of collagen-glycosaminoglycan scaffolds: stromal vascular fraction versus adipose tissue-derived microvascular fragments. *J Biol Eng* 2018; 12: 24.
9. Laschke MW, Karschnia P, Scheuer C, et al. Effects of cryopreservation on adipose tissue-derived microvascular fragments. *J Tissue Eng Regen Med* 2018; 12(4): 1020–1030.
10. Laschke MW, Heß A, Scheuer C, et al. Subnormothermic short-term cultivation improves the vascularization capacity of adipose tissue-derived microvascular fragments. *J Tissue Eng Regen Med* 2019; 13(2): 131–142.
11. Laschke MW, Heß A, Scheuer C, et al. University of Wisconsin solution for the xeno-free storage of adipose tissue-derived microvascular fragments. *Regen Med* 2019; 14(7): 681–691.
12. Karschnia P, Scheuer C, Heß A, et al. Erythropoietin promotes network formation of transplanted adipose tissue-derived microvascular fragments. *Eur Cell Mater* 2018; 35: 268–280.
13. Halberg N, Khan T, Trujillo ME, et al. Hypoxia-inducible factor 1alpha induces fibrosis and insulin resistance in white adipose tissue. *Mol Cell Biol* 2009; 29(16): 4467–4483.

14. Cao Y. Angiogenesis and vascular functions in modulation of obesity, adipose metabolism, and insulin sensitivity. *Cell Metab* 2013; 18(4): 478–489.
15. Lemoine AY, Ledoux S and Larger E. Adipose tissue angiogenesis in obesity. *Thromb Haemost* 2013; 110: 661–668.
16. Gealekman O, Gurav K, Chouinard M, et al. Control of adipose tissue expandability in response to high fat diet by the insulin-like growth factor-binding protein-4. *J Biol Chem* 2014; 289(26): 18327–18338.
17. Okabe M, Ikawa M, Kominami K, et al. "Green mice" as a source of ubiquitous green cells. *FEBS Lett* 1997; 407(3): 313–319.
18. Nakano M, Nakajima Y, Kudo S, et al. Effect of autotransplantation of microvessel fragments on experimental random-pattern flaps in the rat. *Eur Surg Res* 1998; 30(3): 149–160.
19. Stone R II and Rathbone CR. Microvascular fragment transplantation improves rat dorsal skin flap survival. *Plast Reconstr Surg Glob Open* 2016; 4(12): e1140.
20. Shepherd BR, Hoying JB and Williams SK. Microvascular transplantation after acute myocardial infarction. *Tissue Eng* 2007; 13(12): 2871–2879.
21. Pilia M, McDaniel JS, Guda T, et al. Transplantation and perfusion of microvascular fragments in a rodent model of volumetric muscle loss injury. *Eur Cell Mater* 2014; 28: 11–23; discussion 23–24.
22. Orth M, Altmeyer MAB, Scheuer C, et al. Effects of locally applied adipose tissue-derived microvascular fragments by thermoresponsive hydrogel on bone healing. *Acta Biomater* 2018; 77: 201–211.
23. Moreno MJ, Ball M, Andrade MF, et al. Insulin-like growth factor binding protein-4 (IGFBP-4) is a novel anti-angiogenic and anti-tumorigenic mediator secreted by dibutyryl cyclic AMP (dB-cAMP)-differentiated glioblastoma cells. *Glia* 2006; 53(8): 845–857.
24. Li Y, Higashi Y, Itabe H, et al. Insulin-like growth factor-1 receptor activation inhibits oxidized LDL-induced cytochrome C release and apoptosis via the phosphatidylinositol 3 kinase/Akt signaling pathway. *Arterioscler Thromb Vasc Biol* 2003; 23(12): 2178–2184.
25. Hao CN, Geng YJ, Li F, et al. Insulin-like growth factor-1 receptor activation prevents hydrogen peroxide-induced oxidative stress, mitochondrial dysfunction and apoptosis. *Apoptosis* 2011; 16(11): 1118–1127.
26. Wang L, Han Y, Shen Y, et al. Endothelial insulin-like growth factor-1 modulates proliferation and phenotype of smooth muscle cells induced by low shear stress. *Ann Biomed Eng* 2014; 42(4): 776–786.
27. Sabater AL, Andreu EJ, García-Guzmán M, et al. Combined PI3K/Akt and Smad2 activation promotes corneal endothelial cell proliferation. *Invest Ophthalmol Vis Sci* 2017; 58(2): 745–754.
28. Lee KS, Lim BV, Jang MH, et al. Hypothermia inhibits cell proliferation and nitric oxide synthase expression in rats. *Neurosci Lett* 2002; 329(1): 53–56.
29. Drabek T, Tisherman SA, Beuke L, et al. Deep hypothermia attenuates microglial proliferation independent of neuronal death after prolonged cardiac arrest in rats. *Anesth Analg* 2009; 109(3): 914–923.
30. Baeyens N. Fluid shear stress sensing in vascular homeostasis and remodeling: towards the development of innovative pharmacological approaches to treat vascular dysfunction. *Biochem Pharmacol* 2018; 158: 185–191.
31. Galie PA, Nguyen DH, Choi CK, et al. Fluid shear stress threshold regulates angiogenic sprouting. *Proc Natl Acad Sci U S A* 2014; 111(22): 7968–7973.